

UC Berkeley

UC Berkeley Previously Published Works

Title

Liquid-Crystalline Phase Behavior in Polypeptoid Diblock Copolymers

Permalink

<https://escholarship.org/uc/item/2d93s0xz>

Journal

Macromolecules, 51(23)

ISSN

0024-9297

Authors

Greer, Douglas R
Stolberg, Michael A
Xuan, Sunting
[et al.](#)

Publication Date

2018-12-11

DOI

10.1021/acs.macromol.8b01952

Peer reviewed

Liquid-Crystalline Phase Behavior in Polypeptoid Diblock Copolymers

Douglas R. Greer,^{1,2} Michael A. Stolberg,³ Sunting Xuan,³ Xi Jiang,¹ Nitash P. Balsara,^{*†1,2} and Ronald N. Zuckermann^{*‡3}

¹ Materials Sciences Division, Lawrence Berkeley National Laboratory, Berkeley, CA 94720 United States.

² College of Chemistry, University of California, Berkeley, Berkeley, CA 94720 United States.

³ Molecular Foundry, Lawrence Berkeley National Laboratory, Berkeley, CA 94720 United States.

† nbalsara@berkeley.edu

‡ rnzuckermann@lbl.gov

ABSTRACT

Polypeptoid homopolymers and block copolymers undergo thermal transitions in the solid state that can be detected by differential scanning calorimetry (DSC), but so far there is neither consensus on the underpinnings of the observed thermal transitions, nor consensus on the expected number of transitions. We synthesized a series of polypeptoid diblock copolymers containing hydrophobic alkyl sidechains and hydrophilic ethyleneoxide sidechains, systematically varying side-chain length (S), backbone main-chain length (N), block copolymer composition (n/m), and N -terminal group,

and studied their thermal transitions by a combination of X-ray scattering and DSC. The thermal transitions are largely unaffected by S , N , and n/m , but strongly affected by the N -terminal group. Block copolymers with an acetylated N -terminus exhibit two thermal transitions. The low temperature thermal transition is due to a transition from a crystalline phase to a smectic liquid crystalline mesophase. The molecules adopt planar, board-like conformations and are arranged in a rectangular crystal lattice with extended backbones that run parallel to each other. The side-chains extend on either side and are located within the plane of the backbone. The liquid crystalline phase is characterized by conformational disorder in dimensions normal to the molecular plane. The high temperature thermal transition is due to melting of the liquid crystalline phase to give an isotropic phase. Block copolymers with a free N -terminus (non-acetylated) exhibit only one thermal transition, and similar out-of-plane conformational disorder. This disorder appears to be due to a difference in the pendant side chain display angle of the terminal nitrogen atom.

INTRODUCTION

Poly N -substituted glycine polymers (polypeptoids) are a family of comb-like polymers that can be synthesized by either iterative solid-phase synthesis¹⁻³ or conventional solution polymerization.⁴⁻⁷ Polypeptoids are structurally similar to polypeptides, but the absence of hydrogen bond donors along the polypeptoid backbone provides a simplified platform to study polymer

melting behavior. A large number of polypeptoids are crystalline with accessible thermal transitions and exhibit well-defined X-ray diffraction peaks.⁸⁻¹¹ The polypeptoids synthesized by submonomer solid-phase synthesis with sequence-defined and nearly monodispersed features are ideal systems for studying the relationship between molecular structure and crystalline behavior.⁸⁻⁹ Thermal transitions in crystalline polypeptoids have been probed by several investigators,⁸⁻¹¹ but so far there is neither consensus on the underpinnings of the observed thermal transitions, nor on the expected number of transitions. Rosales *et al.* studied the melting of alkyl-substituted polypeptoid homopolymers synthesized by solid-phase synthesis. They used differential scanning calorimetry (DSC) to show that these materials have a single thermal transition, and that their melting temperature and enthalpy decrease as a function of alkyl sidechain length.⁹ Surprisingly, Lee *et al.* observed two melting transitions were observed in high molecular weight alkyl-substituted polypeptoid homopolymers synthesized by solution polymerization.⁸ They attributed the first thermal transition to sidechain melting and the second thermal transition to backbone melting. Fetsch *et al.* also observed two thermal transitions in the DSC measurements of poly *N*-pentyl glycine, and likewise attributed the first thermal transition to crystalline packing of the side chains.¹² Sun *et al.* studied the melting of polypeptoid diblock copolymers synthesized by solid-phase synthesis containing an *N*-decylglycine block (Ndc) and a triethyleneoxy block (Nte).¹⁰ They also observed two thermal transitions,

which were attributed to the melting of the separate Nte and Ndc blocks. It is evident that a comprehensive understanding of thermal transitions in polypeptoids is lacking.

In the present study, we synthesized a systematic series of diblock copolypeptoids, varying side-chain length (S), backbone main-chain length (N), block copolymer composition (n/m), and N -terminal capping group, in order to elucidate the relationship between thermal transitions and molecular structure. The thermal transitions in these materials were studied by a combination of temperature-dependent X-ray scattering and DSC. We show that most of the crystalline polypeptoids in the present study are in fact liquid crystalline, exhibiting a smectic mesophase, a phase previously found in polymers with flexible alkyl side chains emanating from an extended, rigid aromatic backbone.¹³⁻²⁰ This smectic mesophase is characterized by the parallel stacking of board-like molecules, with different spatial arrangements of the stacks. This finding suggests a general framework for understanding thermal transitions in a wide range of polypeptoid materials and nanoassemblies.

EXPERIMENTAL SECTION

Synthesis of polypeptoids. The mPEG amine submonomers 2-(2-methoxyethoxy)ethylamine and 2-(2-(2-methoxyethoxy)ethoxy)ethylamine, for Nde and Nte (mPEG₂-NH₂ and mPEG₃-NH₂), were purchased from PurePEG (98% purity) and Peptide Solutions, Inc. (98% purity), respectively. Linear

alkyl amines and 4-methylpiperidine were purchased from TCI (>98% purity). *N,N'*-diisopropylcarbodiimide was purchased from Chem-Impex International, Inc. ($\geq 99\%$ purity). Bromoacetic acid was purchased from ACROS Organics (99% purity). Trifluoroacetic acid was purchased from Sigma Aldrich (99% purity). All other solvents (HPLC grade) used in this study were purchased from Millipore. All polypeptoids in this study were synthesized using automated solid-phase submonomer synthesis on a Symphony X peptide synthesizer at a scale of 200 mg Rink amide resin (0.64 mmol/g) by adapting reported procedures.²¹⁻²² Bromoacylation reactions were performed with bromoacetic acid (0.8 M) and *N,N'*-diisopropylcarbodiimide (0.8 M) in DMF for 20 min at room temperature. Displacement reactions were performed at 1 M amine concentrations in DMF for 30 min at room temperature. *N*-terminal acetylation of the polypeptoids was performed on the crude, cleaved polypeptoids ((~200 mg) in 2 mL DMF/THF (1:5, v/v), followed by the addition of 100 μ L acetic anhydride and 100 μ L pyridine, and allowed to stir at room temperature for 20 min.²³ The solvents were then removed under vacuum, and the crude product was lyophilized in acetonitrile/water (1:1, v/v). Purification was performed on a reverse phase HPLC Waters prep system equipped with a XSelect HSS cyano column ((5 μ m, 18 x 150 mm) using a linear gradient of 50-95% B in 20 min at a flow rate of 20 mL/min (solvent A is 10% isopropyl alcohol (IPA) in water, and solvent B is 10% IPA in acetonitrile). The collected fractions containing pure product were evaporated and lyophilized from acetonitrile/water (1:1, v/v) to afford a fluffy

white powder. The final product was analyzed by MicroTOF electrospray mass spectrometry and reverse phase HPLC equipped with an analytical cyano column. 50 mg of final product with 80-90%% molecular purity was obtained in most cases.

X-ray scattering. Wide angle X-ray scattering (WAXS) and small angle X-ray scattering (SAXS) measurements were performed at ALS beamline 7.3.3²⁴ and SSRL beamline 1-5. Prior to measurement, lyophilized polypeptoids were placed between Kapton windows separated by a rubber gasket spacer, annealed at 125 °C for half an hour, and cooled slowly to remove thermal history. All polypeptoids synthesized for this study are known to be isotropic above 100 °C.¹⁰⁻¹¹

Differential scanning calorimetry (DSC). Differential scanning calorimetry was performed on a TA Instruments Q2000 series with a nitrogen purge rate of 50 mL/min. The calorimeter was calibrated with an indium reference. Samples of between 2 mg and 10 mg of lyophilized peptoid were loaded into Aluminum T-Zero series pans and compressed with standard lids. An unloaded pan with lid of the same type was used as reference for all samples. To erase thermal history, all samples were first heated from room temperature to 150 °C. The samples were then put through two cycles of cooling to 0 °C and heating to 150 or 180 °C at a rate of 10 °C/min. All data shown is from the second heating cycle with exothermic being up. Labels near each melting peak display the temperature in °C of the enthalpy

extrema and the integrated melting enthalpy in J/g of total polymer. Peaks were integrated using a linear method.

RESULTS AND DISCUSSION

The crystal structure of the *N*-acetylated diblock copolypeptoid family, Ac-Ndc_n-*b*-Nte_m, has been previously studied at room temperature.²² It was shown that these molecules adopt board-like configurations in the crystalline state as shown in Figure 1a. X-ray scattering data from these samples²² contain peaks corresponding to the dimensions *a*, *b*, and *c* shown in Figure 1a. It was shown that *b* is a linear function of backbone length, *c* is a linear function of side chain length, and *a* is independent of these parameters.²² All of the block copolymers exhibited microphase separation in the crystalline state.¹⁰ Here we seek a molecular level understanding of how the chains become disordered upon melting for both *N*-acetylated polypeptoid crystals and their non-acetylated counterparts.

In the acetylated polymers, the *N*-terminal nitrogen atom is *sp*² hybridized (trigonal planar) as are the other nitrogen atoms in the chain. The angle between the *N*-terminal side chain and the backbone is thus expected to be nearly identical to that between internal side chains and the backbone (Figure 1d). In the non-acetylated polymer, the terminal nitrogen atom is *sp*³ hybridized (tetrahedral). In this case, the angle between the *N*-terminal side chain and the backbone is distinct from that between internal side chains

and the backbone (Figure 1e). As we describe below, this small molecular difference has a large impact on the crystallization properties.

A series of *N*-acetylated and non-acetylated polypeptoid block copolymers comprised of alkane and ether-containing *N*-substituted glycine monomers were synthesized by an iterative solid-phase method for this study (Figure 1 and Table 1). In most cases, the polymers were synthesized as matched pairs: each acetylated block copolymer has a non-acetylated counterpart. In block copolymers **1-5**, the acetyl group is directly adjacent to the block with the alkyl side chains. Block copolymers **6-9** are non-acetylated matched pairs of these polymers (except for Ac-Ndc₉-Nte₂₇ (**4**)). The length of the block with alkyl side chains, *n*, and the length of the block with ethyleneoxide side chains, *m*, and side chain length, *S*, were varied over a considerable range (Table 1). The number of monomers in each block is used to define *n* and *m*, while the number of non-hydrogen atoms in the side chain is used to define *S*. In the final four columns of Table 1 are the thermal transition data compiled from our DSC studies.

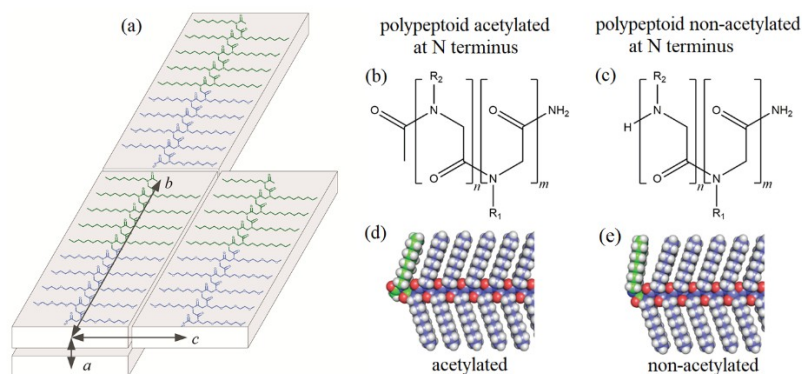
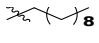
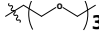
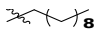
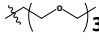
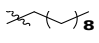
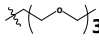
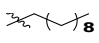
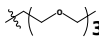
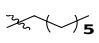
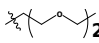
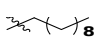
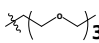
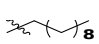
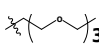
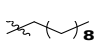
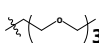
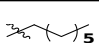
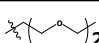


Figure 1. (a) The unit cell and supramolecular assembly of polypeptoid diblock copolymers. Ac-Ndc₉-Nte₉ (**1**) is shown, with the Ndc block in green and the Nte block in blue. The unit cell shown is not perfectly orthorhombic; the angle between *a* and *c* directions is about 95°, as shown in ref. x. Chemical structures for the acetylated (Ac-) (b) and non-acetylated (H-) (c) polypeptoids in Table 1, with *m* side chains R₁ and *n* sidechains R₂. R₁ is di- or tri-ethyleneoxy and R₂ is *n*-decyl or *n*-heptyl. The main-chain length (*N*) listed in Table 1 is equal to *n* + *m*. Geometric structures of the *N*-terminal Ndc monomers in the acetylated (d) and non-acetylated polypeptoids (e).

We first examined the thermal behavior of these polymers in the solid state by DSC. For all these polymers, we found that the acetylated block copolymers (**1-5**) exhibit two thermal transitions at around 45 °C and 90 °C, while the non-acetylated block copolymers (**6-9**) exhibit one thermal transition at around 90 °C (Figure S1-S3). Surprisingly, a subtle change in the end group structure of the diblock copolypeptoids (N-acetylated vs. non-acetylated) results in a significant difference in their thermal behavior. This unexpected phenomenon inspired us to further investigate the impact of the N-terminus on the crystal structures of the diblock copolypeptoids and their thermal transitions.

Table 1: Polypeptoid diblock copolymers synthesized, and their chemistry and heating thermal transitions

	Peptoid Nomenclature	Side chain	Side chain 2	<i>N</i>	<i>S</i>	<i>n</i>	<i>m</i>	<i>T_m</i>		ΔH_m	
								<i>T_m</i> ₁	<i>T_m</i> ₂	ΔH_m ₁	ΔH_m ₂

		1 (R ₁)	(R ₂)					(°C)	(°C)	(J/g)	(J/g)
1	Ac-Ndc ₉ -Nte ₉			1 8	1 0	9	9	45. 6	95. 0	11.9	20.0
2	Ac-Ndc ₉ -Nte ₅			1 4	1 0	9	5	44. 0	87. 0	9.2	17.4
3	Ac-Ndc ₉ -Nte ₁₅			2 5	1 0	9	1 5	45. 8	96. 2	7.2	14.9
4	Ac-Ndc ₉ -Nte ₂₇			3 6	1 0	9	2 7	41. 1	92. 1	4.1	5.1
5	Ac-Nhp ₉ -Nde ₉			1 8	7	9	9	41. 9	96. 6	11.3	21.7
6	H-Ndc ₉ -Nte ₉			1 8	1 0	9	9	-	89. 9	-	16.5
7	H-Ndc ₉ -Nte ₅			1 4	1 0	9	5	-	83. 3	-	19.2
8	H-Ndc ₉ -Nte ₁₅			2 4	1 0	9	1 5	-	87. 4	-	11.7
9	H-Nhp ₉ -Nde ₉			1 8	7	9	9	-	87. 2	-	25.3

“-” denotes not observed.

We next use X-ray scattering to study the structural underpinnings of these thermal transitions. The melting of Ac-Ndc₉-Nte₉ (**1**) crystals, as seen by DSC, exhibits two thermal transitions (Figure 2). At temperatures above the second melting point, (**1**) is an isotropic liquid with no discernible X-ray scattering features. We thus focus on the low temperature thermal transition (Figure 2). In Figure 3, we show the results of three separate X-ray scattering experiments across different scattering angles wherein (**1**) was heated across the first thermal transition. The small-angle X-ray scattering (SAXS) profiles (Figure 3a), which reflect the *b* dimension of the crystal (corresponding to the length of the main chain, Figure 1a), are insensitive to temperature. We thus conclude that the first thermal transition does not affect the length of the polymer chain (*b* ≈ 52 Å). The intermediate-angle X-

ray scattering profiles (Figure 3b), which reflect the c dimension of the crystal (corresponding to the side chain width, Figure 1a) are also insensitive to temperature. In contrast, wide-angle X-ray scattering (WAXS), which reports on the closest packing dimension, a , reveals significant changes as a function of temperature (Figure 3c). At 30 °C, we see the (100) peak corresponding to the a dimension at $q = 1.36 \text{ \AA}^{-1}$. We also see higher order scattering peaks corresponding to (101), (102), and (103) reflections. The presence of these reflections indicates the long-range correlation between the c direction and a direction. With increasing temperature, the (101), (102), and (103) peaks become less pronounced while the (100) peak broadens. At 50 °C, only a single broad peak corresponding to the a dimension at $q = 1.36 \text{ \AA}^{-1}$ is visible in Figure 3c. The average spacing between molecules along the a direction remains unchanged as the temperature changes from 30 to 50 °C. The primary signature of the lower thermal transition is thus due to an increase in disorder along the a direction.

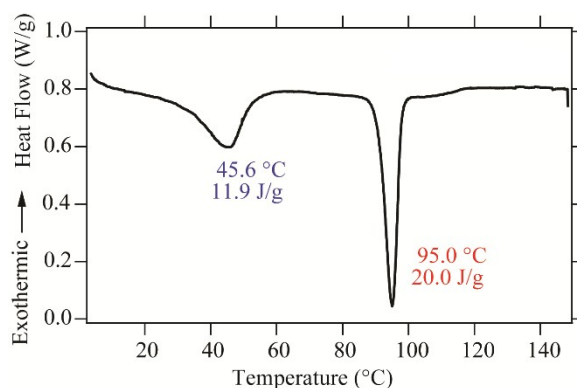


Figure 2. Second heating DSC trace of Ac-Ndc₉-Nte₉ (**1**). Endothermic maxima temperatures and transition enthalpies are displayed.

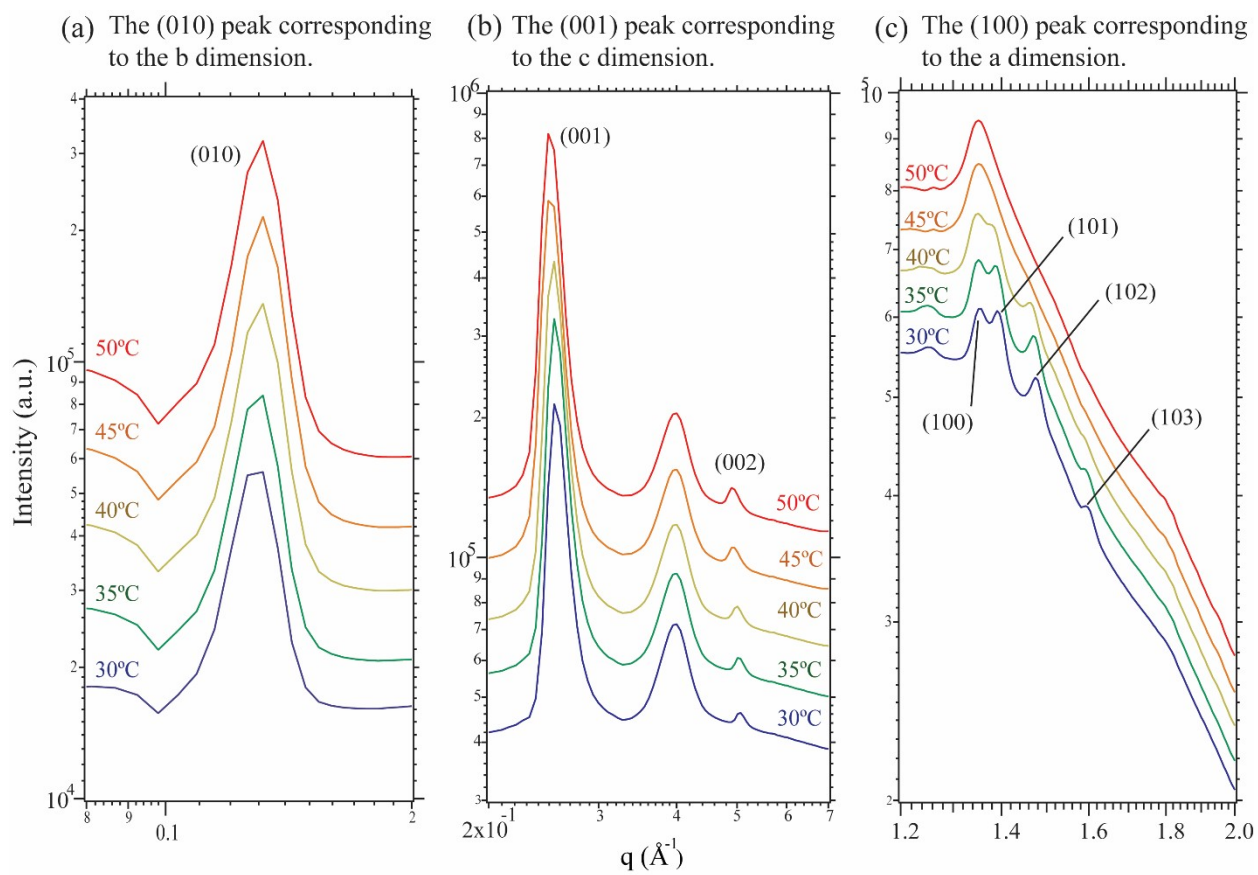


Figure 3. X-ray scattering measurements of Ac-Ndc₉-Nte₉ (**1**) through the first thermal transition. (a) SAXS measurements showing the (010) peak corresponding to the b dimension. (b) WAXS measurements showing the (001) and (002) peaks corresponding to the c dimension. The peak at $q = 0.4 \text{ \AA}^{-1}$ is due to the Kapton windows. (c) WAXS measurements showing the broadening of the (100) peak at $q = 1.36 \text{ \AA}^{-1}$ corresponding to the a dimension, and the loss of the (101), (102) and (103) peaks at higher q .

Our interpretation of the temperature-dependent X-ray scattering data is depicted in Figure 4. At 30 °C, we obtain a simple periodic crystal with aligned molecules as shown in Figure 4a. At 50 °C, beyond the first thermal

transition, the disappearance of the (101), (102), and (103) reflections indicate that the periodicity along the *a* dimension is diminished. Since the *a* dimension represents the closest packing between adjacent molecules (Figure 1a), this implies that the planes of the molecules along the *a* dimension are disordered as shown schematically in Figure 4b. We posit that the polymer exhibits a smectic liquid crystalline mesophase at around 50 °C. This mesophase was first discovered in melts of polymers with alkyl side chains emanating from an aromatic backbone.¹³⁻¹⁴ The distinct signature of this mesophase in our diblock copolypeptoids is a broad X-ray scattering peak characterizing a loss of order along the *a* dimension with no loss of order along the *b* and *c* dimensions (Figure 3, 50 °C). Going back to the DSC data in Figure 2, the first thermal transition at around 50 °C is attributed to the transition from a crystalline structure to a smectic liquid crystalline mesophase. The second thermal transition at 90 °C is attributed to the melting of the smectic mesophase into an isotropic liquid. Heating the samples across the second thermal transition leads to the simultaneous disappearance of all of the X-ray scattering peaks shown in Figure 3 (Figure S4). Since the second thermal transition has been reported before for polypeptoids,¹⁰ we mainly focus here on the nature of the first thermal transition (30-50 °C).

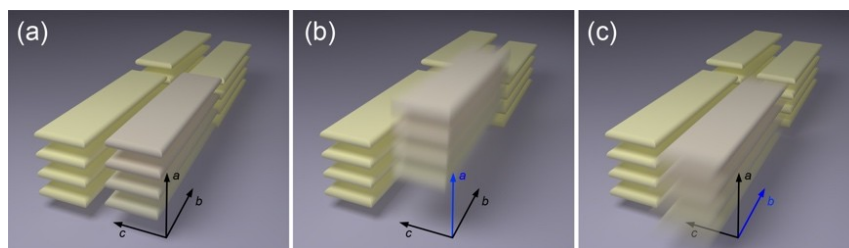


Figure 4. A comparison of ordering in polypeptoid materials in (a), the crystalline phase below T_{m1} and in (b) and (c), in the smectic liquid crystalline mesophase above T_{m1} and below T_{m2} . In the crystalline phase (a), the backbones are extended and parallel to each other. The unit cell of the crystal structure shown in (a) is not perfectly orthorhombic, as shown in ref. x.; the angle between a and c directions is about 95° . In the smectic liquid crystalline mesophase, (b) and (c), the molecules stay aligned in stacks, and molecular distortions are restricted to the ab plane (each mode shown separately, the degree of motion is exaggerated for clarity).

We next examined the impact of N -terminal acetylation. The melting of H-Ndc₉-Nte₉ (**6**) crystals, as seen by DSC, is shown in Figure 5. Unlike its acetylated matched pair, melting in this sample occurs primarily in one step at around 90 °C. The X-ray scattering profiles obtained from the sample at temperatures between 30 and 50 °C are shown in Figure 6. The X-ray scattering profiles of H-Ndc₉-Nte₉ (**6**) are very similar to those of Ac-Ndc₉-Nte₉ (**1**) (compare Figures 3 and 6) in spite of the dramatic differences in the DSC data (compare Figures 2 and 5). Figures 6a and 6b indicate that the b and c dimensions of the crystal are unaffected by temperature changes between 30 and 50 °C. In Figure 6c, we see the disappearance of the (101), (102), and

(103) peaks as temperature increases and the appearance of a single broad (100) peak. There is no difference between the crystal structures of H-Ndc₉-Nte₉ (**6**) and Ac-Ndc₉-Nte₉ (**1**) at 50 °C (compare Figures 6c and 3c). There is, however, a subtle difference between the crystal structures of H-Ndc₉-Nte₉ (**6**) and Ac-Ndc₉-Nte₉ (**1**) at 30 °C: the (101), (102), and (103) peaks of H-Ndc₉-Nte₉ (**6**) are superposed on the broad scattering peak obtained at 30 °C, while those of Ac-Ndc₉-Nte₉ (**1**) are not. It therefore appears that the disorder of the molecular planes along the *a* dimension (Figure 4c), a characteristic of the sanidic liquid crystalline mesophase, seen in Ac-Ndc₉-Nte₉ (**1**) at 50 °C, is present in H-Ndc₉-Nte₉ (**6**) at 30 °C. The disorder of the molecule planes along the *a* dimension at 30 °C suppresses the first thermal transition in H-Ndc₉-Nte₉ (**6**). The qualitative difference in the crystal structure of H-Ndc₉-Nte₉ (**6**) and Ac-Ndc₉-Nte₉ (**1**) described above is seen in most of the matched pairs. This is shown in Figure 7 where we show WAXS data from all of the matched pairs at room temperature. The non-acetylated samples (**6**, **7**, and **8**) all exhibit WAXS peaks superposed on a broad sanidic peak and they exhibit only one thermal transition in the vicinity of 90 °C. Their acetylated counterparts (**1**, **2**, and **3**) all exhibit WAXS peaks that are not superposed on a broad sanidic peak and exhibit two thermal transitions in the vicinity of 40 and 90 °C. Samples **5** and **9** are exceptions. While the WAXS and DSC data from **5** are consistent with the above observations, the WAXS data from the non-acetylated **9** shows one thermal transition but no evidence of a broad

sanidic peak, perhaps due to their shorter side chains which are known to be more highly ordered⁸.

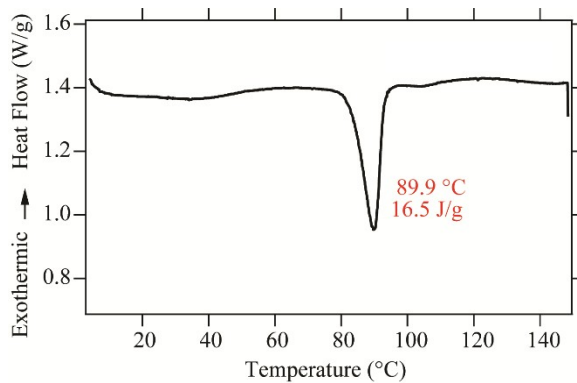


Figure 5. Second heating DSC trace of H-Ndc₉-Nte₉ (**6**). Endothermic maxima temperatures and transition enthalpies are displayed.

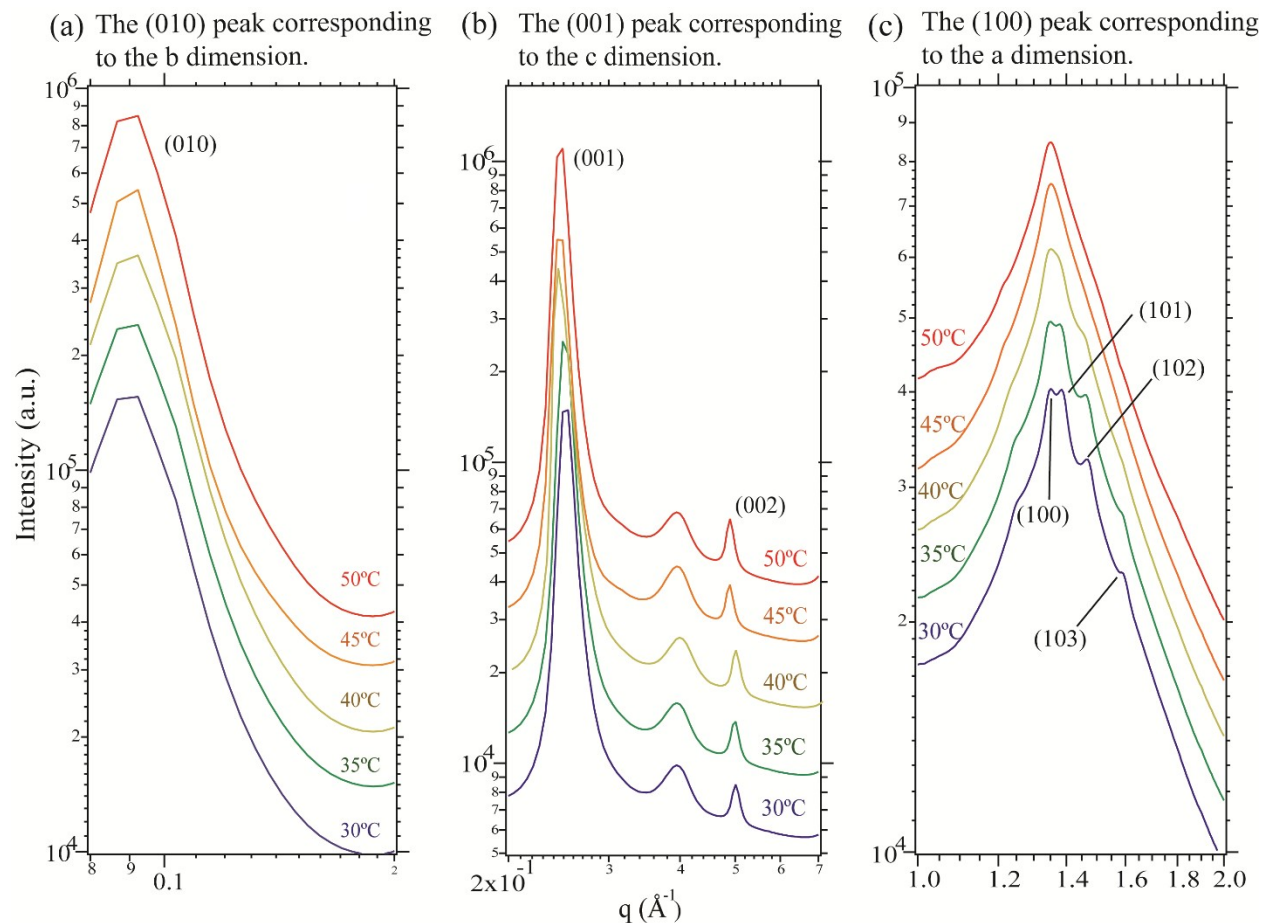


Figure 6. X-ray scattering measurements of H-Ndc₉-Nte₉ (**6**) through the first thermal transition. (a) SAXS measurements showing the (010) peak corresponding to the *b* dimension. (b) WAXS measurements showing the (001) and (002) peaks corresponding to the *c* dimension. The peak at $q = 0.4 \text{ \AA}^{-1}$ is due to the Kapton windows. (c) WAXS measurements showing the broadening of the (100) peak at $q = 1.36 \text{ \AA}^{-1}$ corresponding to the *a* dimension, and the loss of the (101), (102) and (103) peaks at higher q .

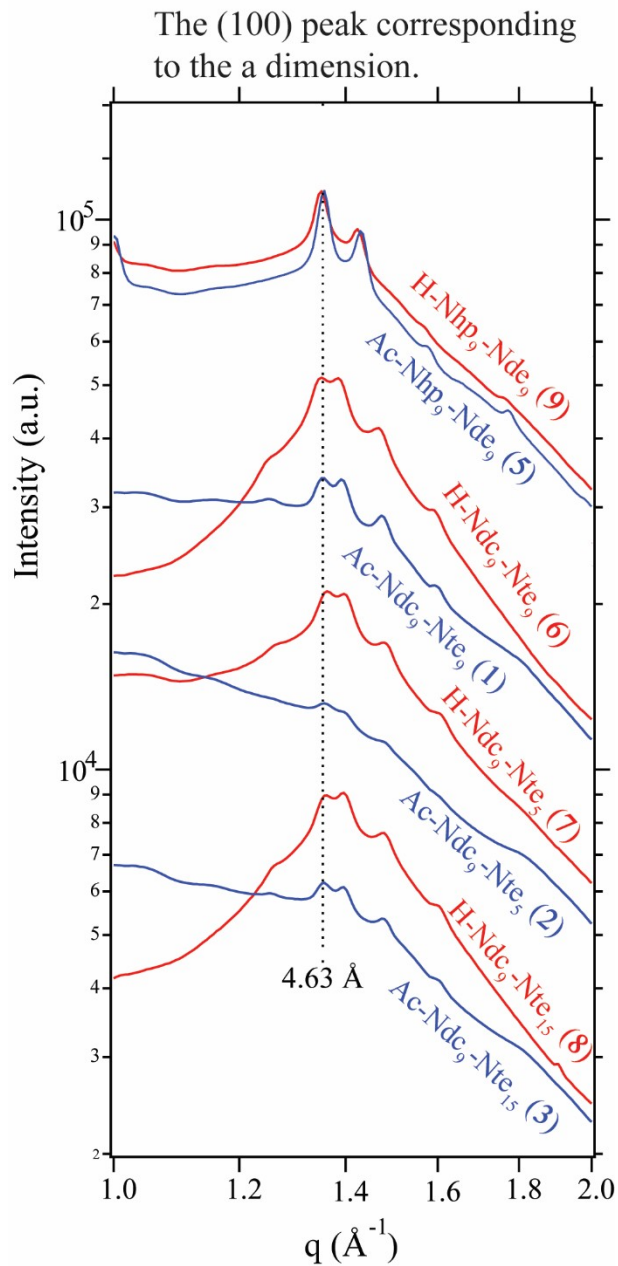


Figure 7. WAXS measurements at high q showing peaks corresponding to a dimension. Intensity is displayed in arbitrary units, and curves are shifted vertically for clarity.

It is clear from the discussion above that the two thermal transitions that are sometimes observed in polypeptoid block copolymers are not associated

with the melting of individual blocks; all of the non-acetylated diblock copolymers exhibit only one thermal transition. Instead, the first thermal transition is associated with the selective loss of order along the *a* dimension while the second thermal transition is associated with the complete loss of order along all dimensions. This phenomenology was only previously observed in branched aromatic polymers with stiff backbones.^{13-14, 16-19} The origin of backbone stiffness in polypeptoids remains an interesting open question. We recently showed that nearly all known crystalline polypeptoids adopt an all-*cis* backbone conformation, suggesting there is a universal low-energy conformation preferred by the peptoid backbone.²² The stiffness and extended structure may arise due to inter-chain interactions along the backbone,²⁵ or it may be induced by packing constraints from the side chains. Direct evidence for this stiffness has been reported using temperature-dependent resonant soft X-ray scattering measurements on similar peptoid diblock copolymers.²⁶ One of the dominant factors for inducing disorder of the molecular planes along the *a* dimension appears to be the orientation of the *N*-terminal side chain as depicted in Figures 1d and e. We propose that the increase disorder along the *a* dimension in the non-acetylated polypeptoid crystals is due to a difference in hybridization of the *N*-terminal nitrogen, resulting in a display angle mismatch of the *N*-terminal side chain (sp^3) relative to the internal side chains (sp^2). Interestingly, the number of thermal transitions (one versus two) and the thermal transition temperatures in the peptoids studied here are mainly affected by the *N*-

terminal group, not the other parameters that define molecular structure: S , N , and n/m .

CONCLUSION

We present a systematic study on the thermal transitions of polypeptoid diblock copolymers with alkyl and ethyleneoxide side chains using DSC and X-ray scattering. We explored the relationship between molecular structure and thermal transitions by varying the side chain length (S), backbone main-chain length (N), block copolymer composition (n/m), and the N -terminal group. Surprisingly, the T_m and ΔH of the thermal transitions are largely unaffected by S , N , and n/m . The nature of the thermal transitions is mainly affected by the N -terminal group. Block copolymers with an acetyl N -terminal group exhibit two thermal transitions. The low temperature thermal transition is due to a transition from a crystalline phase to a smectic liquid crystalline mesophase. The polypeptoids adopt board-like molecular conformations in the crystalline phase. The *cis* backbones of polypeptoids in the crystal are extended and parallel to each other. The liquid crystalline phase is characterized with the selective loss of planar order along the a dimension. The high temperature thermal transition is due to melting of the liquid crystalline phase. A broad X-ray scattering peak in the vicinity of $q = 1.4 \text{ \AA}^{-1}$ is a signature of the smectic liquid crystalline phase in these diblock copolypeptoids. Block copolymers with a hydrogen atom at the N -terminus exhibit only one thermal transition. At low temperatures, the higher order

scattering peaks corresponding to the crystalline phase in these block copolymers are superposed on the broad scattering peak that is the signature of the smectic phase. This indicates that the molecular conformations in these crystals are characterized by planar disorder along the *a* dimension. We posit that the difference in the angle between the *N*-terminal side chain and the backbone and that between the internal side chains and the backbone cause conformational disorder of the molecules along the *a* dimension.

ACKNOWLEDGMENT

The work was funded primarily by the Soft Matter Electron Microscopy Program (KC11BN), supported by the Office of Science, Office of Basic Energy Science, US Department of Energy, under Contract DE-AC02-05CH11231. Work at the Molecular Foundry, the Advanced Light Source and the High Performance Computing Services Group at Lawrence Berkeley National Laboratory was supported by the Office of Science, Office of Basic Energy Science, US Department of Energy, under Contract DE-AC02-05CH11231. Use of the Stanford Synchrotron Radiation Lightsource, SLAC National Accelerator Laboratory, is supported by the U.S. Department of Energy, Office of Science, Office of Basic Energy Sciences under Contract No. DE-AC02-76SF00515. We gratefully acknowledge Dr. Ryan Spencer for his discussions on peptoid assembly and Dr. Satyendra Kumar and Dr. Chunhui Bao for their discussions on liquid crystalline phases.

SUPPORTING INFORMATION

DSC traces of diblock copolypeptoids, heating WAXS and heating SAXS measurements of diblock copolypeptoids, and characterization data of diblock copolypeptoids. This material is available free of charge via the Internet at <http://pubs.acs.org>.

AUTHOR INFORMATION

Corresponding Authors

*nbalsara@berkeley.edu; rnzuckermann@lbl.gov

Notes

The authors declare no competing financial interest.

References

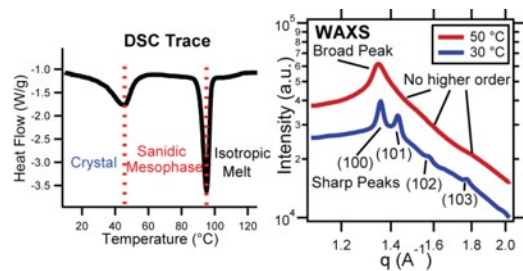
- (1) Zuckermann, R. N.; Kerr, J. M.; Kent, S. B. H.; Moos, W. H. Efficient method for the preparation of peptoids [oligo(N-substituted glycines)] by submonomer solid-phase synthesis. *J. Am. Chem. Soc.* **1992**, *114* (26), 10646-10647.
- (2) Sun, J.; Zuckermann, R. N. Peptoid Polymers: A Highly Designable Bioinspired Material. *ACS Nano* **2013**, *7* (6), 4715-4732.
- (3) Zuckermann, R. N. Peptoid origins. *Pept. Sci.* **2011**, *96* (5), 545-555.
- (4) Chan, B. A.; Xuan, S.; Li, A.; Simpson, J. M.; Sternhagen, G. L.; Yu, T.; Darvish, O. A.; Jiang, N.; Zhang, D. Polypeptoid polymers: Synthesis, characterization, and properties. *Biopolymers* **2017**, e23070.
- (5) Gangloff, N.; Ulbricht, J.; Lorson, T.; Schlaad, H.; Luxenhofer, R. Peptoids and Polypeptoids at the Frontier of Supra- and Macromolecular Engineering. *Chem. Rev.* **2016**, *116* (4), 1753-1802.
- (6) Zhang, D.; Lahasky, S. H.; Guo, L.; Lee, C.-U.; Lavan, M. Polypeptoid Materials: Current Status and Future Perspectives. *Macromolecules* **2012**, *45* (15), 5833-5841.
- (7) Secker, C.; Brosnan, S. M.; Luxenhofer, R.; Schlaad, H. Poly(α -Peptoid)s Revisited: Synthesis, Properties, and Use as Biomaterial. *Macromol. Biosci.* **2015**, *15* (7), 881-891.

- (8) Lee, C.-U.; Li, A.; Ghale, K.; Zhang, D. Crystallization and Melting Behaviors of Cyclic and Linear Polypeptoids with Alkyl Side Chains. *Macromolecules* **2013**, *46* (20), 8213-8223.
- (9) Rosales, A. M.; Murnen, H. K.; Zuckermann, R. N.; Segalman, R. A. Control of Crystallization and Melting Behavior in Sequence Specific Polypeptoids. *Macromolecules* **2010**, *43* (13), 5627-5636.
- (10) Sun, J.; Teran, A. A.; Liao, X.; Balsara, N. P.; Zuckermann, R. N. Crystallization in Sequence-Defined Peptoid Diblock Copolymers Induced by Microphase Separation. *J. Am. Chem. Soc.* **2014**, *136* (5), 2070-2077.
- (11) Sun, J.; Jiang, X.; Lund, R.; Downing, K. H.; Balsara, N. P.; Zuckermann, R. N. Self-assembly of crystalline nanotubes from monodisperse amphiphilic diblock copolypeptoid tiles. *Proc. Natl. Acad. Sci.* **2016**, *113* (15), 3954-3959.
- (12) Fetsch, C.; Luxenhofer, R. Thermal Properties of Aliphatic Polypeptoids. *Polymers* **2013**, *5* (1), 112.
- (13) Voigt-Martin, I. G.; Simon, P.; Bauer, S.; Ringsdorf, H. Structure and Defects in Sanidic Liquid Crystalline Polymers. 1. *Macromolecules* **1995**, *28* (1), 236-242.
- (14) Voigt-Martin, I. G.; Simon, P.; Yan, D.; Yakimansky, A.; Bauer, S.; Ringsdorf, H. Structure and Defects in Sanidic Liquid Crystalline Polymers. 2. Structure Analysis of Sanidic Polymers by Simulation of Diffraction Patterns from Monomeric Analogs. *Macromolecules* **1995**, *28* (1), 243-254.

- (15) Windle, A. H. Structure of Thermotropic Main-Chain Polymers. In *Liquid Crystalline and Mesomorphic Polymers*; 1st Ed.; Shibaev, P. V.; Lam, L., Eds. Springer: New York, 2014; pp 26-76.
- (16) Rodriguez-Parada, J. M.; Duran, R.; Wegner, G. A comparative study of mesophase formation in rigid-chain polyesters with flexible side chains. *Macromolecules* **1989**, *22* (5), 2507-2516.
- (17) Repasky, P. J.; Agra-Kooijman, D. M.; Kumar, S.; Hartley, C. S. Smectic-A and Hexatic-B Liquid Crystal Phases of Sanidic Alkyl-Substituted Dibenzo[fg,op]naphthalenes. *J. Phys. Chem. B* **2016**, *120* (10), 2829-2837.
- (18) Galda, P.; Kistner, D.; Martin, A.; Ballauff, M. Characterization and analysis of the phase behavior of poly(1,4-phenylene 2,5-di-n-alkoxyterephthalates). *Macromolecules* **1993**, *26* (7), 1595-1602.
- (19) Sone, M.; Harkness, B. R.; Kurosu, H.; Ando, I.; Watanabe, J. Rigid-Rod Polyesters with Flexible Side Chains Based on 1,4-Dialkyl Esters of Pyromellitic Acid and 4,4'-Biphenol. 5. High-Resolution ¹³C NMR Studies for Crystalline and Liquid Crystalline Layered Phases. *Macromolecules* **1994**, *27* (10), 2769-2777.
- (20) Ebert, M.; Herrmann-Schönherr, O.; Wendorff, J. H.; Ringsdorf, H.; Tschirner, P. Sanidics: A new class of mesophases, displayed by highly substituted rigid-rod polyesters and polyamides. *Liq. Cryst.* **1990**, *7* (1), 63-79.

- (21) Au - Tran, H.; Au - Gael, S. L.; Au - Connolly, M. D.; Au - Zuckermann, R. N. Solid-phase Submonomer Synthesis of Peptoid Polymers and their Self-Assembly into Highly-Ordered Nanosheets. *JoVE* **2011**, (57), e3373.
- (22) Greer, D. R.; Stolberg, M. A.; Kundu, J.; Spencer, R. K.; Pascal, T.; Prendergast, D.; Balsara, N. P.; Zuckermann, R. N. Universal Relationship between Molecular Structure and Crystal Structure in Peptoid Polymers and Prevalence of the cis Backbone Conformation. *J. Am. Chem. Soc.* **2018**, *140* (2), 827-833.
- (23) Kim, S.; Biswas, G.; Park, S.; Kim, A.; Park, H.; Park, E.; Kim, J.; Kwon, Y.-U. Unusual truncation of N-acylated peptoids under acidic conditions. *Org. Biomol. Chem.* **2014**, *12* (28), 5222-5226.
- (24) Hexemer, A.; Bras, W.; Glossinger, J.; Schaible, E.; Gann, E.; Kirian, R.; MacDowell, A.; Church, M.; Rude, B.; Padmore, H. A SAXS/WAXS/GISAXS Beamline with Multilayer Monochromator. *J. Phys. Conf. Ser.* **2010**, *247* (1), 012007.
- (25) Edison, J. R.; Spencer, R. K.; Butterfoss, G. L.; Hudson, B. C.; Hochbaum, A. I.; Paravastu, A. K.; Zuckermann, R. N.; Whitelam, S. Conformations of peptoids in nanosheets result from the interplay of backbone energetics and intermolecular interactions. *Proc. Natl. Acad. Sci.* **2018**, *115* (22), 5647-5651.
- (26) Kortright, J. B.; Sun, J.; Spencer, R. K.; Jiang, X.; Zuckermann, R. N. Oxygen K Edge Scattering from Bulk Comb Diblock Copolymer Reveals

Extended, Ordered Backbones above Lamellar Order-Disorder Transition. *J. Phys. Chem. B* **2017**, *121* (1), 298-305.



TOC Graphic